Chapter 5

Synthesis, spectroscopic characterization, Hirshfeld surface analysis and crystal structure of Silver (4-Amino-N-(2-pyrimidinyl)benzenesulfonamide, pyridine

5.1. Introduction

Sulfadiazine (SDZ), 4-Amino-N-(2-pyrimidinyl) benzenesulfonamide, is a significant member of 'sulfa family'. Sulfadiazine has been used to control acute infections when studying murine models of reactivated toxoplasmosis. It eliminates bacteria that cause infection by stopping the production of folate inside the bacterial cell, and is commonly used to treat urinary tract infections, and burns **[202].** In combination, sulfadiazine and pyrimethamine can be used to treat toxoplasmosis, a disease caused by Toxoplasma gondii **[203].** It is well known that sulfadiazine is a useful antibacterial drug with the typical sulfonamide structure. It is on the World Health Organization's List of Essential Medicines, the most important medications needed in a basic health system **[204]**. This finding has aroused considerable interest and great efforts have been made to design new antitumor agents by combining sulfadiazine with other antitumor agents as one compound. The chemical structure of sulfadiazine is shown in **Figure 5.1**.

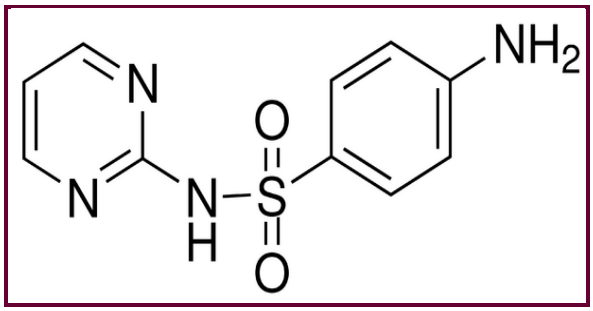

Figure 5.1 Chemical structure of sulfadiazine

The X-ray crystal structure of sulfadiazine is initially reported for the first time by Shin et al. **[205]** in 1974. The first crystal structure of AgSDZ is determined by Cook et al. **[172-a]** in 1975 and in 1976, the same crystal structure is also reported by Baenziger et al. **[172-b]**. Few metal complexes of sulfadiazine such as copper **[206]**, zinc **[207-208],** mercury **[209]** and cadmium **[210]** complexes of sulfadiazine have been reported earlier.

In this chapter, author has attempted to explore the synthesis, spectral characterization, X-ray crystal structure, Hirshfeld surface analysis and quantum chemical calculations of silver complex of sulfadiazine. In these types of complexes, the coordination is often expected via either of the three nitrogen atoms of amino, sulfonamido and pyrimidine **[172-b]**. To explore

the geometry and stereochemistry of new complex, different spectral techniques such as IR and ^{1}H NMR are used. The quantum chemical study of optimized molecular geometries and Mulliken population are examined. The optimized geometric parameters are calculated using Schrodinger software by B3LYP method. Comparison of the experimental geometric parameters and theoretical one indicated that all optimized bond lengths and angles are in good agreement. The 3D Hirshfeld surface analysis and 2D fingerprint analysis are performed to understand the role of the interactions and their quantitative contributions towards the stability of molecular packing. To correlate structure-function relationship, biological response of the AgSDZ is examined against gram negative and gram positive bacteria.

5.2.Experimental

5.2.1. Chemicals

Sulfadiazine is procured from Sigma-Aldrich and all solvent are purchased from Loba-Chemie. The silver nitrate and solvents are reagent grade and used without further purification.

5.2.2. Synthesis of Silver Complex of Sulfadiazine

Sodium salt of sulfadiazine (0.545g, 2 mmol) is dissolved in hot methanol and to this, an aqueous solution of silver nitrate ($AgNO_3$) (0.1689 gm, 1mmol) is added with constant stirring and the mixture is refluxed for 2 hours. A white precipitate is formed, filtered and washed with hot distilled water and methanol consecutively and dried in a desiccator over anhydrous $CaCl_2$. The yield at the end of reaction is around 45%. The results for [2($AgC_{10}H_9N_4O_2S$] are: Anal. Calcd. (%): C, 33.79; H, 2.64; N, 14.94. Found (%): C, 41.30; H, 3.23; N, 16.05.

5.3. Spectroscopic Characterization

5.3.1. IR Spectroscopy

To confirm the presence of coordination of metal with the ligand, the IR spectra of the free ligand and the metal complex are studied (**Figure 5.2** and **Figure 5.3**) and assigned on the basis of careful comparison of their spectra with that of free ligand. The infrared (IR) spectra

are recorded in the region 4000-400 cm^{-1} using KBr pallet. The probable assignments for particular stretching frequencies are tabulated in **Table 5.1**.

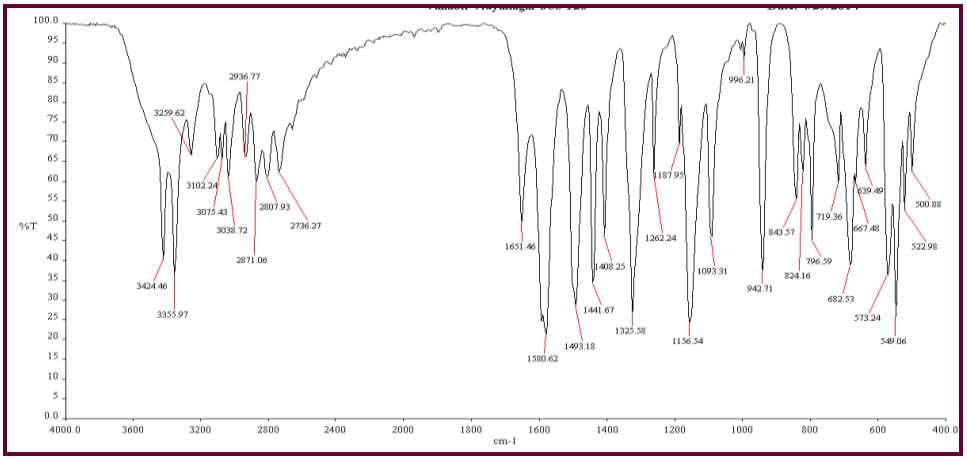

Figure 5.2 FTIR spectra of SDZ

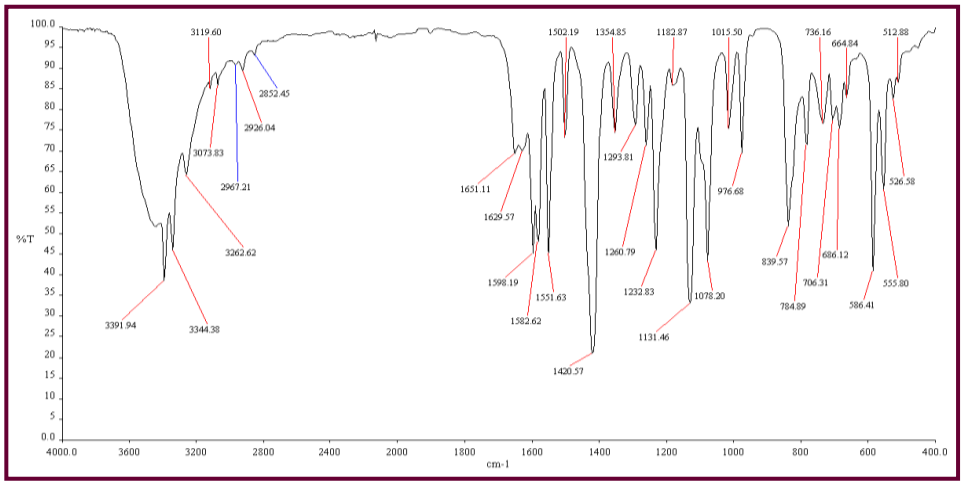

Figure 5.3 FTIR spectra of AgSDZ

The bands appear at 3391 and 3344 cm^{-1} due to $\nu_{as}(NH_2)$ and $\nu_{sy}(NH_2)$ vibrations of the amino ($–NH_2$) group are modified in the spectra of silver complex in comparison to that of the free sulfadiazine ligand. These modifications are most probably due to the hydrogen bonding between complex involving the NH_2 and SO_2 groups. The peak for the sulfonamidic (N–H) group in the free sulfadiazine ligand at around 3038 cm^{-1}, is remained absent in the spectra of the AgSDZ, confirming the deprotonation of the $–SO_2NH–$ moiety. The scissoring vibrations for the amino ($–NH_2$) groups appear at 1651 cm^{-1} whereas peaks due to phenyl ring appear at around 1582 and 1598 cm^{-1} in both the spectra. The peaks around 1325 and 1262 cm^{-1} are

assigned to $\nu_{as}(SO_2)$ shift to 1293 and 1260 cm^{-1}, and those at 1156 cm^{-1} to $\nu_{sy}(SO_2)$ shift to 1131 cm^{-1} due to complexation. The band in the sulfadiazine ligand at 996 and 942 cm^{-1} is assigned to ν(S–N) and are at higher frequencies (976–1078 cm^{-1}) in the spectra of complex, as a consequence of coordination to the metal. These shifts to higher frequencies are in accordance with the shortening of the S–N bond length.

Table 5.1 Characteristic IR bands (cm^{-1}) of the spectra of SDZ (1) and AgSDZ (2) complex

Assignment	(1)	(2)
N–H	3038	---
$\nu as(NH_2)$	3424	3391
$\nu s(NH_2)$	3355	3344
$\delta(NH_2)$	1651	1651
ν-phenyl ring	1580, 1493	1598, 1582
$(SO_2)as$	1325, 1262	1293, 1260
$(SO_2)sy$	1156	1131
ν(S–N)	996, 942	1078, 976

5.3.2. ^{1}H NMR Spectroscopy

The ^{1}H NMR spectrum of the AgSDZ are recorded in DMSO-d_6[a] and compared with that of the ligand. The chemical shifts are expressed in ppm relative to internal TMS. The ^{1}H NMR assignments of sulfadiazine and its silver complex are summarized in **Table 5.2.** ^{1}H NMR spectra of sulfadiazine and its Ag-sulfadiazine are presented in **Figure 5.4** and **Figure 5.5** respectively.

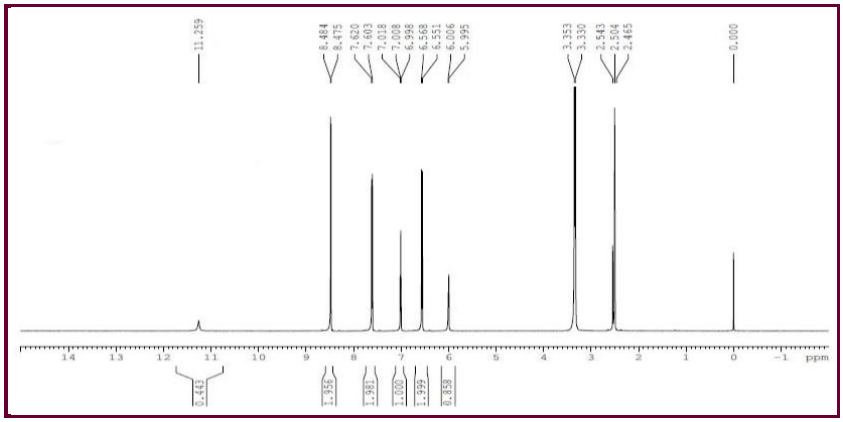

Figure 5.4 ^{1}H NMR spectra of SDZ

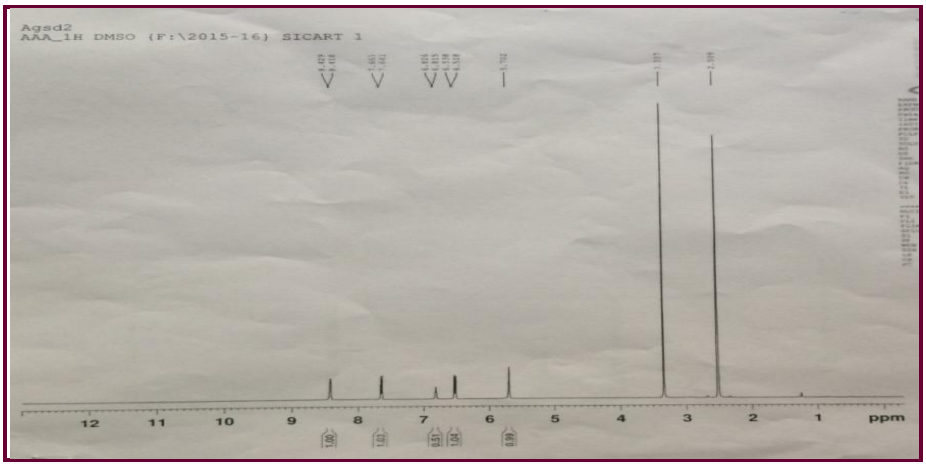

Figure 5.5 ^{1}H NMR spectra of AgSDZ

Almost all of ^{1}H NMR resonance suffers up field shift. The signals for hydrogen bonded to aromatic carbon are almost comparable in ligand and in complex: H3 & H5; 6.56 ppm in SDZ, 6.43 ppm in AgSDZ ($\Delta\delta$ = -0.13 ppm). H2&H4; 7.62 ppm in SDZ, 7.66 ppm in AgSDZ ($\Delta\delta$ = -0.04 ppm). H9; 7.00 ppm in SDZ and 6.82 ppm in the complex ($\Delta\delta$ = -0.18 ppm). The most noticeable observation is for signal of amide proton (N1-H, δ= 9.880 ppm) which may be attributed to electron sharing between Ag ion and nitrogen in the ^{1}H NMR spectrum of the complex.

Table 5.2 ^{1}H NMR shift assignments of SDZ (1) and its AgSDZ (2) in DMSO-d_6[a]

Assignment	^{1}H(1)	^{1}H(2)	$\Delta\delta$(H)[b]
N(1)–H	11.25	----	----
C(8)–H/C(10)-H	8.48	8.41	-0.07
C(9)-H	7	6.82	-0.18
C(2)–H/C(6)-H	7.62	7.66	0.04
C(3)–H/C(5)-H	6.56	6.43	-0.13
NH_2	6	5.7	-0.3

[a]Relative to TMS with DMSO-d_6 peak as reference (^{1}H, 2.60 ppm, ^{13}C,43.5 ppm)
[b]$\Delta\delta$ = δ(sulfonamide complex) - δ(sulfonamide)

5.4. X-ray Crystallographic Investigation

Transparent plate shaped diffraction quality single crystals are grown by slow evaporation technique using pyridine. A transparent crystal with size (0.30 × 0.08 × 0.04 mm) has been selected for three dimensional X-ray intensity data collection. The photograph of grown single

crystal from pyridine solvent is shown in **Figure 5.6**. Crystallographic data are collected on a Enraf Nonius CCD4 Diffractometer (Smart Apex-II) with graphite monochromated MoK_α radiation ($\lambda = 0.71073$ Å) at CSMCRI, Bhavnagar. The cell refinement and data reduction are carried out using NRCVAX **[211]** programme. In total, data for 9359 reflections have been collected in the range $-10 \leq h \leq 11$; $-14 \leq k \leq 14$; and $-10 \leq l \leq 21$, out of which 3376 reflections found to satisfy the criteria $I > 2\sigma(I)$ and used for further structure solution and refinement purpose. Multi-scan absorption corrections are applied up to $T_{min} = 0.684$ and $T_{max} = 0.947$. Preliminary crystallographic data and refinement parameters are listed in **Table 5.3 and Table 5.4** respectively.

Figure 5.6 Photograph of grown single crystals

Table 5.3 Preliminary Crystallographic Data

Chemical name	:	Silver (4-Amino-N-(2-pyrimidinyl) benzenesulfonamide, pyridine
Chemical formula	:	$2(Ag\ C_{10}H_9N_4O_2S{\cdot}C_5H_5N)$
Molecular weight	:	872.48amu
Crystal system	:	Monoclinic
Space group	:	$P2_1/c$
a	:	8.7146(8) Å
b	:	11.5221(11) Å
c	:	16.4934(16) Å
α	:	90°
β	:	96.34(1)°
γ	:	90°
Volume (V)	:	1646.0(3) $Å^3$
Z	:	4
ρ_c Mg/m^3	:	1.760
μ mm^{-1}	:	1.37
F(000)	:	872

Table 5.4 Intensity Data Collection and Refinement Parameters

Instrument used	:	Bruker SMART APEX-II CCD4 diffaractometer
Temperature during data collection	:	273 K
Size of the crystal	:	0.30 × 0.08 × 0.04 mm
Radiation type	:	MoKα
Radiation source	:	Fine-focus sealed tube
Wavelength (λ)	:	0.71073 Å
Mode of data collection		ω - 2θ scan mode
θ range for data collection (°)	:	θ_{min} = 2.2°, θ_{max} = 28.2°
Total number of measured reflections	:	9359
Total number of independent reflections	:	3573
h	:	-10 to 11
k	:	-14 to 14
l	:	-10 to 21
Refinement method	:	Full Matrix Least Square of $\|F\|^2$
Number of parameters	:	217
Goodness of fit on $\|F\|^2$	:	1.36
Final R indices [I > 2σ(I)]	:	R_1 = 0.047, wR_2 = 0.123
R indices (all data)	:	R_1 = 0.053, wR_2 = 0.137
Largest difference peak and hole	:	$\Delta\rho_{min}$ = -0.92 eÅ^{-3}: $\Delta\rho_{max}$ = 1.03 eÅ^{-3}
Software used to data collection	:	Bruker SMART Apex-II
Software used to cell refinement	:	NRCVAX
Software used to solve the structure	:	SHELXS–97
Software used to refine the structure	:	SHELXL–97
Software used for Molecular Graphics	:	PLUTON and ORTEP-3

5.4.1. Structure Solution and Refinement

Crystal structure of $[(AgC_{10}H_9N_4O_2S{\cdot}C_5H_5N)]_2$ is solved by direct method using SHELXS-97. SHELXS-97 built in WinGX programme package is used to determine the phases to locate the atomic positions and SHELXL97 is used for refinement of the data to obtain a precise

model of the structure. The value of Rint = 0.026 and Rsigma = 0.032. SHELXS-97 parameters of the set which could give the correct solution of the structure are

Filter =0.038 NQUAL = -0.690 CFOM =0.301

R(ALPHA) =0.133 M(ABS) = 0.763

Structure is refined using SHELXL-97 programme package which uses Full-Matrix least-square refinement method. Initially, a value of 0.05 is assigned as the isotropic temperature factor to each non-hydrogen atoms. Few cycles of isotropic thermal refinement of the positional parameters of the non-hydrogen atoms and followed by anisotropic refinement for couple of cycles for non-hydrogen atoms reduced final residual index to $R[F^2 > 2\sigma(F^2)] = 0.047$. The hydrogen atoms are stereochemically positioned with C-H = 0.93 Å (for aromatic C-H) and N-H = 0.97 Å (terminal amino N-H) and refined with the riding model to their parent atoms with $U_{iso}(H) = 1.2\ U_{eq}$ (carrier atoms of CH, NH). All the non hydrogen atoms are refined anisotropically by full-matrix least squares procedure against F^2. The model is refined by full-matrix least squares on F^2 with SHELXL-97. The final weighting scheme is $W = 1/[\sigma^2(F_o^2)+(0.0613P)^2 + 2.0776P]$ where $P=(F_o^2+2F_c^2)/3$ with goodness of fit S = 1.36. Highest and lowest electron density peaks '$\Delta\rho$' are 1.03 and -0.96 $eÅ^{-3}$ respectively. The final positional parameters of non-hydrogen atoms for molecule of Ag sulfadiazine complex and pyridine with equivalent isotropic thermal parameters are listed in **Table 5.5**. **Table 5.6** summarizes the positional co-ordinate of hydrogen atoms with isotropic thermal parameters. The anisotropic thermal parameters of non-hydrogen atoms are given in **Table 5.7**.

Table 5.5 Fractional co-ordinates of the non-hydrogen atoms and equivalent isotropic displacement parameters (Å^2) with estimated standard deviation in parentheses

$$\mathrm{Ueq} = \frac{1}{3}(U11 + U22 + U33)$$

Atom	x	y	z	U_{eq}
Ag1	0.63487(4)	0.51555(3)	–0.04302(2)	0.02809(2)
		Sulfadiazine		
S1	0.79383(2)	0.7361 (9)	0.05973(7)	0.0219(2)
O1	0.8155(3)	0.8233(3)	–0.00089(2)	0.0271(7)
O2	0.9019(4)	0.6389(3)	0.0623(2)	0.0307(8)
N1	0.6276(4)	0.6746(3)	0.0489(2)	0.0218(7)
N2	0.3632(4)	0.6779(3)	0.0293(2)	0.0226(8)
N3	0.5013(4)	0.8568(3)	0.0510(2)	0.0259(8)
N4	0.8893(5)	0.9495(4)	0.3898(2)	0.0298(9)
C1	0.8233(5)	0.8010(4)	0.1574(3)	0.0221(9)
C2	0.8501(5)	0.7307(4)	0.2252(3)	0.0265(9)
C3	0.8748(5)	0.7784(4)	0.3022(3)	0.0282(2)
C4	0.8744(5)	0.8988(4)	0.3119(3)	0.0254(9)
C5	0.8525(6)	0.9688(4)	0.2428(3)	0.0279(2)
C6	0.8242(5)	0.9204(4)	0.1662(3)	0.0262(9)
C7	0.4958(5)	0.7402(4)	0.0433(2)	0.0203(8)
C8	0.2309(5)	0.7391(4)	0.0179(3)	0.0295(2)
C9	0.2265(5)	0.8583(4)	0.0209(3)	0.0324(2)
C10	0.3670(5)	0.9138(5)	0.0397(3)	0.0324(2)
		Pyridine		
N5	0.4832(5)	0.6154(4)	–0.1462(3)	0.0315(9)
C11	0.5049(6)	0.7277(5)	–0.1615(3)	0.0374(2)
C12	0.4125(7)	0.7882(5)	–0.2208(4)	0.0442(3)
C13	0.2956(7)	0.7295(6)	–0.2677(3)	0.0451(4)
C14	0.2748(7)	0.6131(6)	–0.2530(3)	0.0442(3)
C15	0.3696(6)	0.5609(5)	–0.1918(3)	0.0395(2)

Table 5.6 Fractional co-ordinates of hydrogen atoms and isotropic displacement parameters (Å^2)

Atom	**x**	**y**	**z**	**U_{iso}**
Sulfadiazine				
H2	0.8515	0.6505	0.2188	0.032
H3	0.8918	0.7304	0.3477	0.034
H4A	0.941	1.0236	0.3864	0.036
H4B	0.9563	0.9004	0.426	0.036
H5	0.857	1.049	0.2483	0.034
H6	0.8058	0.9679	0.1206	0.031
H8	0.1383	0.6988	0.0074	0.035
H9	0.1344	0.8993	0.0109	0.039
H10	0.3679	0.9942	0.0446	0.039
Pyridine				
H11	0.5851	0.7667	–0.1311	0.045
H12	0.4286	0.8669	–0.2290	0.053
H13	0.2324	0.7679	–0.3083	0.054
H14	0.1982	0.571	–0.2840	0.053
H15	0.3536	0.4827	–0.1814	0.047

Table 5.7 Anisotropic displacement parameters (Å^2) of non-hydrogen atoms with estimated standard deviation in parentheses

Atom	U^{11}	U^{22}	U^{33}	U^{12}	U^{13}	U^{23}
Ag1	0.0278(2)	0.0190(2)	0.0373(2)	–0.00341(2)	0.00292(5)	0.00002(4)
Sulfadiazine						
S1	0.0167(5)	0.0235(5)	0.0256(5)	–0.0009(4)	0.0030(4)	–0.0038 (4)
O1	0.0224(5)	0.0355(8)	0.0245(6)	–0.0055(3)	0.0071(2)	0.0014 (4)
O2	0.0184(5)	0.0347(9)	0.0401(9)	0.0086(3)	0.0077(3)	–0.0073(5)
N1	0.0162(6)	0.0212(8)	0.0283(9)	–0.0013(4)	0.0029(4)	–0.0035(5)
N2	0.0236(8)	0.0160(7)	0.028(2)	–0.0028(3)	0.0019(5)	0.0022(4)
N3	0.0225(8)	0.0197(8)	0.036(2)	0.0001(4)	0.0079(6)	0.0025(6)
N4	0.027(2)	0.038(2)	0.025(2)	–0.0035(7)	0.0036(6)	–0.0101(7)
N5	0.029(2)	0.033(2)	0.032(2)	–0.0041(7)	0.0031(7)	0.0027(8)
C1	0.0144(8)	0.028(2)	0.025(2)	–0.0007(6)	0.0038(6)	–0.0032(8)
C2	0.025(2)	0.022(2)	0.032(2)	–0.0020(7)	0.0017(8)	0.0023(8)
C3	0.029(2)	0.031(2)	0.025(2)	–0.0019(9)	0.0014(8)	0.0026(9)
C4	0.018(2)	0.032(2)	0.026(2)	–0.0022(7)	0.0027(6)	–0.0034(9)
C5	0.029(2)	0.022(2)	0.032(3)	–0.0006(7)	0.0030(9)	–0.0052(9)
C6	0.027(2)	0.022(2)	0.030(2)	0.0000(7)	0.0008(8)	0.0025(8)
C7	0.021(2)	0.023(2)	0.0178(9)	–0.0037(6)	0.0064(5)	–0.0003(6)
C8	0.021(2)	0.038(3)	0.031(2)	–0.0028(9)	0.0058(8)	0.006(2)
C9	0.017(2)	0.036(3)	0.045(3)	0.0068(8)	0.0095(9)	0.013(2)
C10	0.031(3)	0.024(2)	0.042(3)	0.0029(9)	0.008(2)	0.008(2)
Pyridine						
C11	0.030(3)	0.040(3)	0.041(3)	0.003(2)	0.004(2)	0.002(2)
C12	0.052(3)	0.033(3)	0.048(3)	0.004(2)	0.009(3)	0.013(3)
C13	0.043(3)	0.058(4)	0.033(3)	0.010(3)	0.000(2)	0.004(3)
C14	0.041(3)	0.057(4)	0.034(3)	–0.002(3)	–0.001(2)	0.000(3)
C15	0.036(3)	0.042(3)	0.039(3)	–0.010(2)	0.001(2)	0.002(2)

5.4.2. Crystal Structure of $[(AgC_{10}H_9N_4O_2S{\cdot}C_5H_5N)_2]$

Silver complex of sulfadiazine crystallizes in monoclinic space group $P2_1/c$ with Z= 4 The geometry at the silver center is a distorted pentadentant. An 'ORTEP' view of the molecule indicating atomic numbering scheme (thermal ellipsoids drawn at 50% probability level) per asymmetric unit is shown in the **Figure 5.7. Figure 5.8** is the geometry of the $(AgC_{10}H_9N_4O_2S{\cdot}C_5H_5N)_2$ showing pentadentant coordination at the silver.

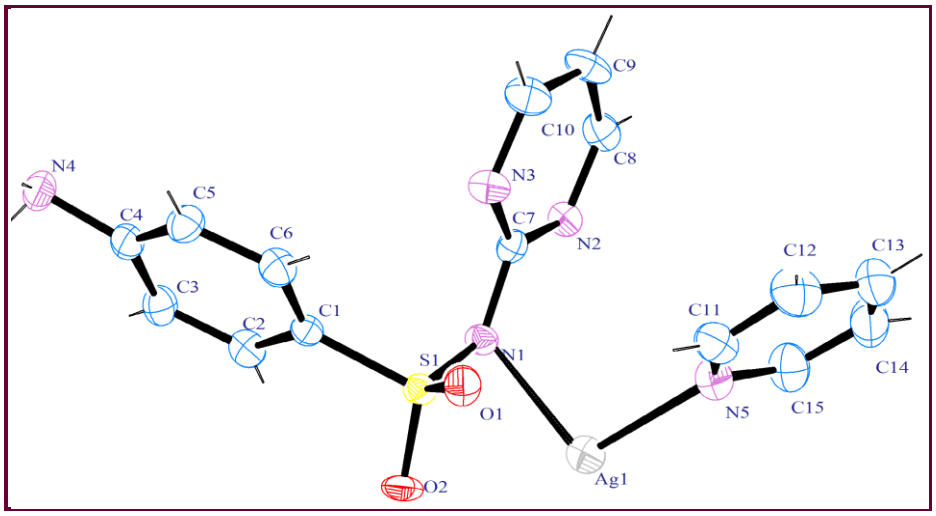

Figure 5.7 ORTEP diagram of the title compound showing thermal displacement ellipsoids are drawn at 50% probability level

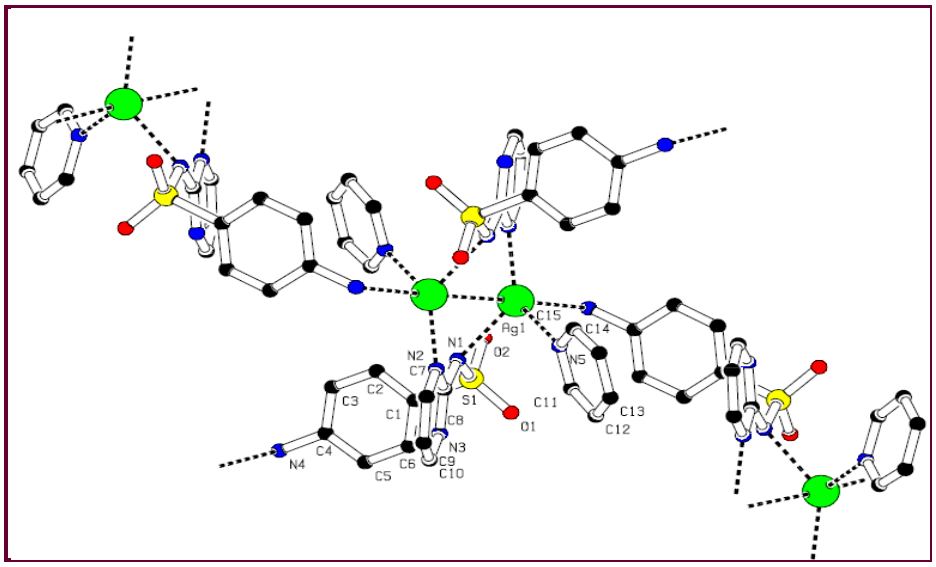

Figure 5.8 Geometry of the $[AgC_{10}H_9N_4O_2S{\cdot}C_5H_5N]_2$. Hydrogen atoms are excluded for better clarity.

Molecular Dimension

All the geometrical calculations are performed using PLATON software. Bond length involving non-hydrogen atoms, as obtained by X-ray data (with estimated standard deviation in parentheses) and by theoretical calculations at the B3LYP /LAV2p** level of theory, are summarized in **Table 5.8 and Table 5.9** tabulates the bond length for hydrogen atoms as obtained by X-ray data. **Table 5.10** presents the bond angle involving non hydrogen atoms as

obtained by X-ray data and by theoretical calculation at the B3LYP/LAV2p** level of theory. The bond length and bond angle of the phenyl ring confirm well to those found in the free sulfadiazine **[203]**. The distances S1–N1 of 1.605(3) Å and N1–C7 of 1.369(5) Å of this complex are comparable with those of other reported silver complexes in literature **[172-174]** and in Chapter 3 and chapter 4 of the thesis. The maximum and minimum values of angle around the sulfur atom are for O1-S1-O2 (114.8(2)˚) and O2-S1-N1 (103.6(2)˚) respectively.

Table 5.8 Bond length (Å) involving non-hydrogen atoms with estimated standard deviation in parentheses as obtained by X-ray data and by B3LYP /LAV2p level of theory**

Bond length	**X-ray**	**B3LYP**	**Bond length**	**X-ray**	**B3LYP**
S1—O1	1.445(3)	1.547	C1—C2	1.379(6)	1.390
S1—O2	1.462(3)	1.581	C1—C6	1.383(6)	1.390
S1—N1	1.605(3)	1.743	C2—C3	1.380(6)	1.390
S1—C1	1.769(4)	1.841	C4—C3	1.397(7)	1.408
N1—C7	1.369(5)	1.360	C4—C5	1.392(7)	1.408
N2—C7	1.359(5)	1.354	C5—C6	1.377(7)	1.389
N2—C8	1.347(6)	1.329	C8—C9	1.375(7)	1.396
N3—C10	1.337(6)	1.329	C10—C9	1.386(7)	1.393
N4—C4	1.404(6)	1.390			
Pyridine					
N5—C11	1.335(7)	1.348	C13—C12	1.386(8)	1.392
N5—C15	1.333(6)	1.344	C13—C14	1.378(9)	1.395
C11—C12	1.384(7)	1.394	C15—C14	1.371(8)	1.394

Table 5.9 Bond length (Å) involving hydrogen atoms as obtained from X-ray data

Bond length	X-ray	Bond length	X-ray
N4—H4A	0.97	C6—H6	0.93
N4—H4B	0.97	C8—H8	0.93
C2—H2	0.93	C9—H9	0.93
C3—H3	0.93	C10—H10	0.93
C5—H5	0.93		
Pyridine			
C11—H11	0.93	C14—H14	0.93
C12—H12	0.93	C15—H15	0.93
C13—H13	0.93		

Table 5.10 Bond angle (°) involving non-hydrogen atoms with estimated standard deviation in parentheses as obtained by X-ray data and that of by B3LYP /LAV2p level of theory**

Bond angle	X-ray	B3LYP	Bond angle	X-ray	B3LYP
O1—S1—O2	114.8(2)	117.70	C1—C2—C3	120.5(4)	118.93
O1—S1—N1	114.6(2)	115.27	C1—C6—C5	119.8(4)	118.79
O1—S1—C1	108.6(2)	108.90	C2—C3—C4	119.9(4)	120.52
O2—S1—N1	103.6(2)	99.05	C2—C1—S1	118.9(3)	118.74
O2—S1—C1	105.6(2)	105.38	C2—C1—C6	120.1(4)	122.06
N1—S1—C1	109.0(2)	109.78	C3—C4—C5	118.9(4)	119.00
N1—C7—N2	114.3(4)	113.90	C4—C5—C6	120.7(4)	120.69
N1—C7—N3	121.5(4)	120.97	C6—C1—S1	121.0(4)	119.20
N2—C7—N3	124.2(4)	125.12	C7—N1—S1	120.3(3)	120.43
N2—C8—C9	123.0(4)	123.40	C7—N3—C10	117.0(4)	116.40
N3—C10—C9	122.9(5)	123.36	C7—N2—C8	116.5(4)	116.26
N4—C4—C3	121.1(4)	120.50	C8—C9—C10	116.2(4)	115.46
N4—C4—C5	119.9(4)	120.47			
		Pyridine			
N5—C11—C12	122.5(5)	122.25	C11—N5—C15	117.5(5)	118.51
N5—C15—C14	123.9(5)	122.84	C12—C13—C14	118.7(5)	118.83
C11—C12—C13	118.9(5)	118.99	C13—C14—C15	118.4(5)	118.58

Co-ordination Sphere of Ag

In crystal structure of the AgSDZ complex, five coordinated distorted pentadented geometry of silver is formed through three nitrogen atoms from three sulfadiazine ligands, one nitrogen atom from pyridine molecule and another symmetry related silver. The Ag-Ag distance is 2.8922(8) which is compatible with other reported silver complexes **[172-175]**. The bond length (**Table 5.11**) involving Ag—N, are compatible to those (2.240-2.617Å) reported in other Ag complexes.

The coordination sphere of silver is formed by aryl amine N4, sulfonamido N1 and pyrimidine N2 from three symmetry related ligand molecules and pyridine nitrogen atom N5 from solvent molecule. The nearly pentadentate bonds on silver present variable distances: Ag1—N1=2.384(4), Ag1—$N2^{ii}$ =2.240(4), Ag1—$N4^{iii}$ =2.617(4) and Ag1—N5 = 2.339(4) Å. The maximum and minimum values of the angle around Ag (I) atom are 175.5(9)° ($N4^{iii}$—Ag1—$Ag1^{ii}$) and 72.8(9)° (N1—Ag1—$Ag1^{ii}$).

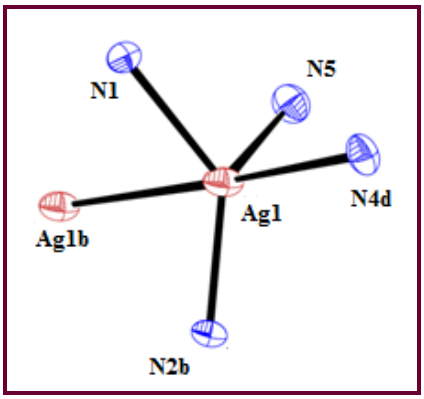

Table 5.11 Coordination covalent geometry surrounding silver

Coordination bond length (Å)			
Ag1—N2^{ii}	2.240(4)	Ag1—N1	2.384(4)
Ag1—N5	2.339(4)	Ag1—N4^{iii}	2.617(4)
Ag1—Ag1^{ii}	2.899(8)		
Coordination bond angle (°)			
N2^{ii}—Ag1—N5	124.1 (4)	N1—Ag1—N4^{iii}	103.5(3)
N2^{ii}—Ag1—N1	134.5(3)	N2^{ii}—Ag1—Ag1^{ii}	79.9(9)
N5—Ag1—N1	91.8(4)	N5—Ag1—Ag1^{ii}	89.6(2)
N2^{ii}—Ag1—N4^{iii}	101.5(4)	N1—Ag1—Ag1^{ii}	72.8(9)
N5—Ag1—N4^{iii}	93.04(3)	N4^{iii}—Ag1—Ag1^{ii}	175.5(9)

Symmetry codes: (i) *x*, –*y*+3/2, *z*+1/2; (ii) –*x*+1, –*y*+1, –*z*; (iii) *x*, –*y*+3/2, *z*–1/2.

Molecular Conformation

The equation of few significant least-square planes, along with the displacement of the relevant atoms from the mean planes and the dihedral angle between the different mean planes are presented in **Table 5.12**. Molecular conformation, described by few torsional angles about significant bonds obtained by X-ray data (with estimated standard deviation in parentheses) and by quantum chemical calculation (B3LYP/LAV2p** levels of theory), is tabulated in **Table 5.13**. Molecule of the complex adopts *cis* conformation about the S—N bond with torsional angle of 68.44 (2)° and it is of 71.07° by theoretical calculation. Pyrimidine ring (C7-N2-C8-C9-C10-N3) and the phenyl ring are effectively planar. Our observation for dihedral angle reflects the fact that pyrimidine ring plane (C7-N2-C8-C9-C10-

N3) is oriented at 74.55(6)° to (C1-C6) phenyl ring plane and by B3LYP method, it is 66.91˚.

Table 5.12 Equation of least-square planes along with the displacement of relevant atoms and the dihedral angle between different planes with standard deviation in parentheses

(1) C1-C2-C3-C4-C5-C6			
0.9972(1) x - 0.0140(18) y - 0.0733(18) z = 0.446(11)			
C1	0.007(4)	C4	0.013(4)
C2	-0.010(4)	C5	-0.017(4)
C3	0.000(4)	C6	0.006(4)
(2) N2-N3-C7-C8-C9-C10			
-0.194(2) x + 0.0614(19) y + 0.9791(4) z = 6.785(14)			
N2	-0.014(3)	C8	-0.008(5)
N3	-0.010(5)	C9	0.020(5)
C7	0.024(5)	C10	-0.012(5)
(3) N5-C11-C12-C13-C14-C15			
0.7113(16) x + 0.237(2) y – 0.6619(17) z = -4.34(3)			
N5	0.004(5)	C13	0.002(6)
C11	-0.010(5)	C14	-0.008(6)
C12	0.007(6)	C15	0.006(5)

Dihedral angle (˚) between LSQ- planes		
Planes	**X-ray**	**B3LYP**
C1-C2-C3-C4-C5-C6 & C7-N2- C8-C9-C10-N3	74.6(2)˚	69.91˚

Table 5.13 Few significant torsional angles (°) with estimated standard deviation in parentheses

Atom	**X-ray**	**B3LYP**	**Atom**	**X-ray**	**B3LYP**
C1 -S1-N1 -C7	68.4(4)	71.07	O1-S1-C1-C2	-162.6(3)	147.7
O1 -S1 -N1 -C7	-53.5(4)	-52.32	N1 -S1-C1-C2	71.9(4)	85.18

5.4.3. Hydrogen Bonding and Molecular Packing

Analysis of the hydrogen bonding pattern shows the presence of π···π, C–H···O and N–H···O intermolecular hydrogen bond interactions in the structure. The intermolecular hydrogen bond interactions are summarized in **Table 5.14**.

Table 5.14 Intermolecular interactions and symmetry code

Hydrogen bond geometry					
D—H···A	H···A Å	D···A Å	∠ D—H···A °		
N4–H4A ···O2 (i)	2.02	2.84(2)	149		
N4–H4 B···O2 (ii)	2.39	3.014(2)	123		
C8 –H8···O2(iii)	2.44	3.24(2)	145		
π ···π intermolecular interaction					
Cg(I)···Cg(J)	Cg(I)···Cg(J)Å	α	B	γ	Cg(J) ···P Å
Cg(2)···Cg(3)(iv)	4.234	40.4	31.1	9.4	-3.6256(19)
Cg(2) and Cg(3) represent the centroid of pyridine ring (N5-C11-C12-C13-C14-C15) and phenyl ring (C1- C6) respectively					
Symmetry code: (i)-x,1/2+y,1/2-z; (ii) x,1/2-y,-1/2+z; (iii) 1+x,y,z; (iv) x,1/2-y,1/2+z.					

In N4–H4A···O2 and N4–H4B···O2 intermolecular hydrogen bonds formed by the sulfonyl oxygen O2 from two symmetry related molecules, acts as an acceptor to terminal amino nitrogen such that N4–H4A···O2=2.896(5) Å with ∠N4–H4A···O2=149° at -x,1/2+y,1/2-z and N4–H4B···O2 = 3.014(5) Å with ∠N4–H4B···O2=123° at x,1/2-y,-1/2+z. Molecular packing diagram displaying N–H···O interactions are elucidated in **Figure 5.9**.

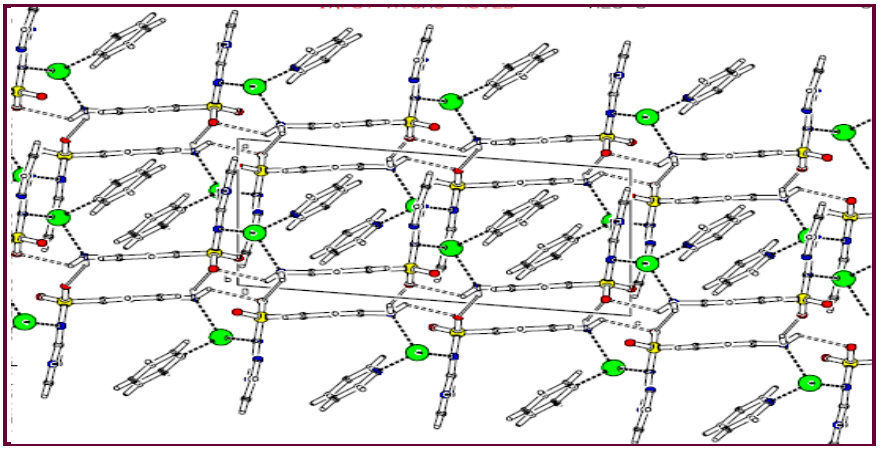

Figure 5.9 A Part of molecular packing diagram showing N4–H4A···O2 and N4–H4B···O2 intermolecular interactions

The molecular packing is further strengthened by π···π interaction, depicted in **Figure 5.10**. The π···π interaction observed between the centroids of the solvent pyridine ring to symmetry related phenyl ring (C1-C6) at x,1/2-y,1/2+z with their centroids separated by 4.23(3) Å.

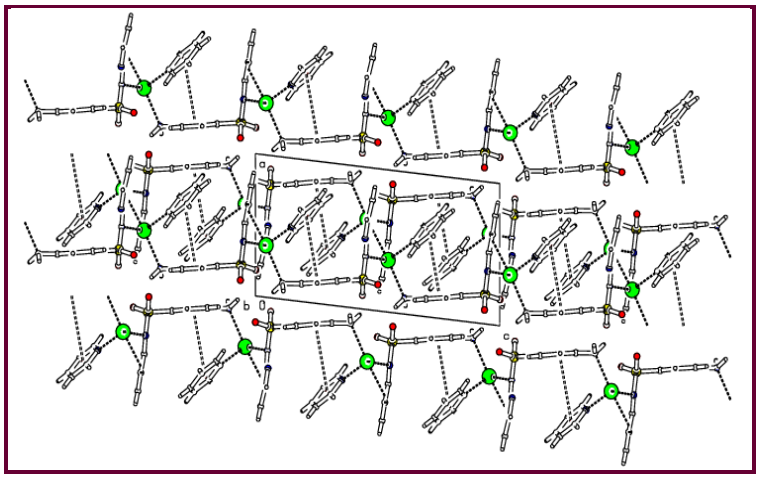

Figure 5.10 Depiction of part of molecular packing of π··· π intermolecular interaction

5.5. Ab – initio and DFT Calculations

Density Functional theory method is used to calculate all quantum chemical calculations performed using JAGUAR utility from Schrodinger software package. The optimization geometry, Mulliken Charge Distribution, dipole moment and HOMO-LUMO calculation have been done using B3LYP method at LAV2p** basis set.

5.5.1. Geometry Optimization Calculations

The optimized geometric parameters, calculated using B3LYP/LAV2p** method, are listed in **Table 5.8** and **Table 5.9**. Comparison between the experimental bond length and theoretical bond length reveals that all optimized data are slightly larger than the experimental value. This is the case because the experimental data are collected in the solid phase, whereas the computational theoretical data corresponded to the isolated molecule in gas phase. The correlation coefficient and root mean square error (RMSE) for molecular geometry (bond length and bond angle) have been calculated and the results are depicted graphically in **Figure 5.11.** The highest bond length and bond angle difference is observed 0.138 Å for the S1—N1 bond and 4.59° for O2—S1—N1 angle. The root mean square error and correlation coefficient values for bond length are 0.047Å and 0.942 respectively, while for bond angle, root mean square error and correlation coefficient are 1.23° and 0.951 respectively.

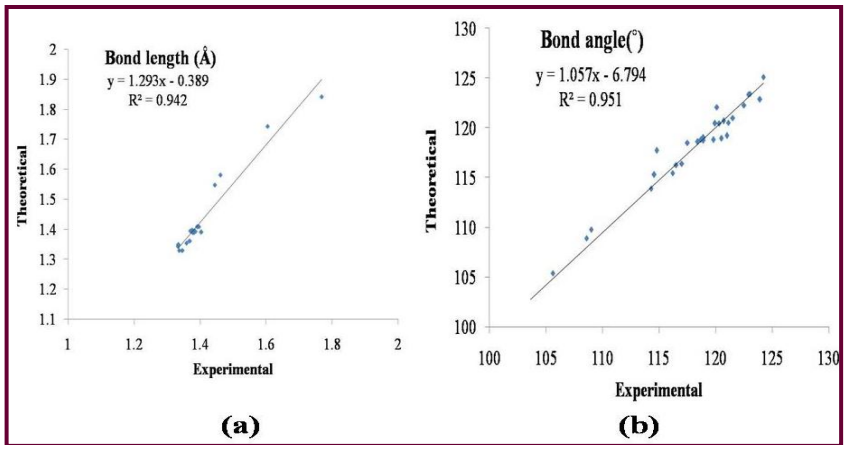

Figure 5.11 Graphical representation of correlation between experimental versus theoretical (a) bond length and (b) bond angle

5.5.2. Mulliken Charge Distributions

The Mulliken charge distribution has been calculated using B3LYP method with LAV2p** level as tabulated in **Table 5.15** and graphically as shown in **Figure 5.12**. It is noted that the all oxygen and nitrogen atoms have negative charge and all hydrogen atoms have positive charge. The sulfonyl oxygen O2 atom has more negative charge (-0.80875) than other oxygen atoms, whereas the hydrogens from amino nitrogen H4A (0.25956) and H4B (0.25853) have almost equal maximum positive charge than the other hydrogen atoms. The sulfonamido nitrogen atom N1 has more negative charge (-0.83322) compare to amino and pyrimidine nitrogen atoms. The results suggest that the oxygen atoms act as electron acceptor and charge transfer takes place from H to O.

Table 5.15 Mulliken charges (e) for atoms calculated by B3LYP method

Atom	Charge	Atom	Charge	Atom	Charge	Atom	Charge
C4	0.24481	C9	-0.13036	H5	0.09341	C13	-0.05235
N4	-0.59567	H9	0.08186	C2	-0.01015	H13	0.11564
H4A	0.25956	Ag1	0.49239	H2	0.14031	C14	-0.09373
H4B	0.25853	S1	1.65211	N5	-0.44349	H14	0.1105
C10	0.08652	C11	0.0949	C6	0.0149	C12	-0.09955
H10	0.09069	H11	0.19033	H6	0.15357	H12	0.11888
N3	-0.40738	O2	-0.80875	C3	-0.14488	C5	-0.14947
C7	0.5869	O1	-0.73992	H3	0.09083	H8	0.09056
N2	-0.40487	C1	-0.34711	C15	0.08522	H15	0.1218
C8	0.0867	N1	-0.83322				

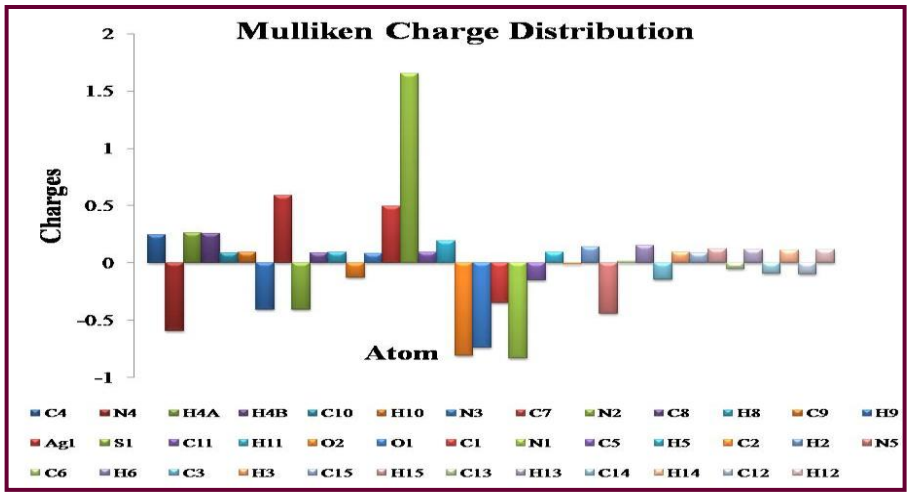

Figure 5.12 Graph sheet of Mulliken atomic charges (e) by B3LYP method

5.5.3. HOMO and LUMO Analysis

HOMO and LUMO energies have been calculated by using B3LYP/ LAV2p** method. The HOMO and LUMO plot are shown in **Figure 5.13**. It is shown that HOMO delocalized on the pyrimidine and sulfonyl nitrogen atom and LUMO is on pyridine ring. The calculated energy value of HOMO is -5.2234 eV and LUMO is -1.51867 eV. The energy gap of HOMO-LUMO (-3.70537eV) explains the charge transfer interaction within the molecule. The value of dipole moment (6.3976 Debye) suggests the reactivity and attraction for the interaction with other system.

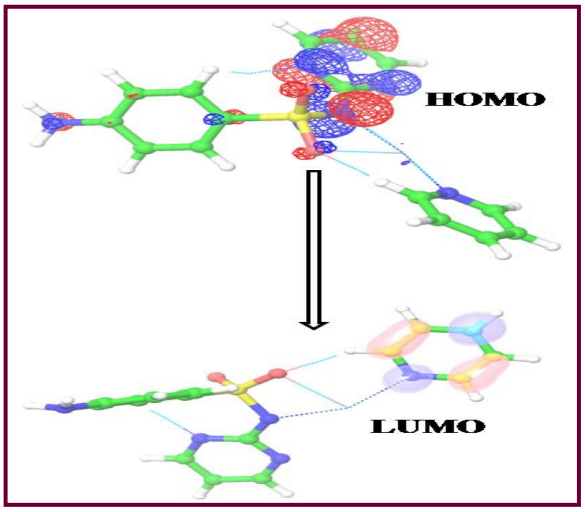

Figure 5.13 The highest occupied molecular orbital (HOMO) and the lowest unoccupied molecular orbital (LUMO) of the molecule

5.6. Hirshfeld Surface Analysis and 2-D Fingerprint Plot

Hirshfeld surfaces are mapped with different properties e.g. de, d_{norm}, shape index, curvedness. The d_{norm} region mapped over -0.631(red) - 1.424 (blue)Å while the shape index region and curvedness region vary from -1.000 to +1.000 Å and -4.000 to +0.400 respectively. The molecular Hirshfeld surface (dnorm, shape index and curvedness) is shown in **Figure 5.14**.

The d_{norm} surface is used for identification of very close intermolecular interactions. In d_{norm} surfaces, the large red circular depressions are the indicators of close hydrogen bonding contacts whereas other visible spots are due to H···H contacts. The presence of red spots on the d_{norm} surface indicate the presence of C–H···O and N–H···O interactions (**Figure 5.14(a)**). Inspection of the shape index and curvedness indicate the presence of C···C interaction between the molecular pairs. The large flat region delineated by a blue outline on curvedness surface refers to the π…π stacking interactions. The curvedness of the present compound indicates π…π stacking interactions (marked with circular region, **Figure 5.14(b &c))**.

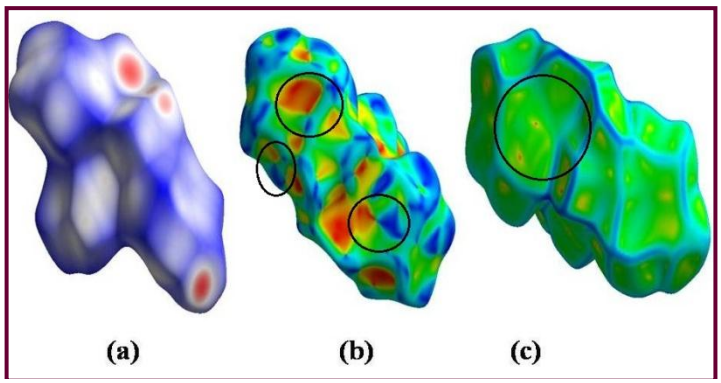

Figure 5.14 Molecular Hirshfeld representing (a) d_{norm} surface (b) shape index surface (c) curvedness surface

The 2-D fingerprint plots complement the Hirshfeld surfaces which are elucidated in **Figure 5.15**. The full fingerprint plot (**Figure 5.15(a))** has been decomposed to emphasize particular atom pair close contacts. This decomposition facilitates the separation of contributions from diverse interaction types, which overlap in the full fingerprint (**Figure 5.15(b)**). The analysis for the fingerprint for all interaction reveals that the outer spikes corresponds to H···O interaction. The H···O contacts can be attributed to C–H···O and N–H···O hydrogen bond interactions, having the 16.7% contribution to the total Hirshfeld surface. Since nitrogen

atoms are coordinating with silver atoms, contribution of H···N contacts, of 6.0 % to the total Hirshfeld surface, is very less. The Hirshfeld surface analysis show a proportion of π···π stacking interactions having contribution of 4.4% of the total Hirshfeld surface. The H···C contacts are indicated by the ‘‘wings’’ in the 2D fingerprint plot and the percentage contribution of this contact is 15.4% of the total Hirshfeld surface.

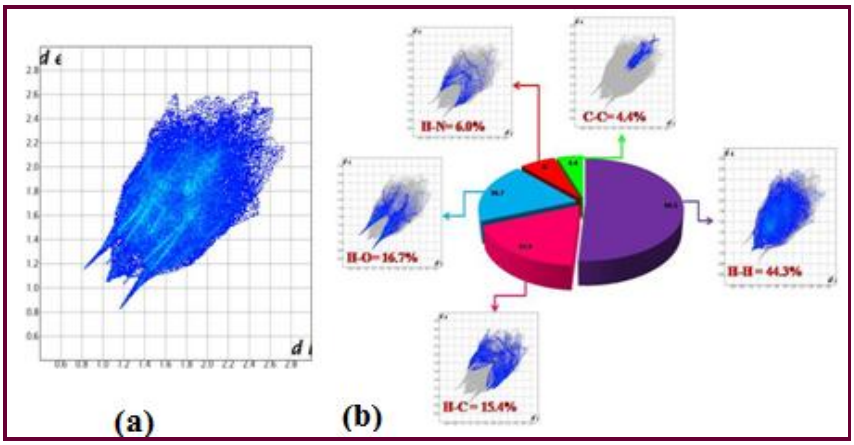

Figure 5.15 (a) 2-D full fingerprint plot (b) decomposition of full fingerprint plot into various contacts

5.7. Microbiological Assay

The minimum inhibitory concentration (MIC) values of sulfadiazine and its silver complex AgSDZ against gram positive and gram negative strains are shown in **Table 5.16**. Sulfadiazine and AgSDZ exhibit varying inhibitory effect towards the bacterial strains. In comparison to sulfadiazine, the silver complex AgSDZ is showing more sensitivity towards both gram negative bacteria (*E. coli & Sh.Flexneri*) and gram positive bacteria (*S. Aureus*), while it shows less activity against Gram-positive bacteria (*B. Subtills*), compare to ligand with same experimental conditions.

Table 5.16 MIC value (µg/ml) of SDZ and AgSDZ

Minimum Inhibition Concentration					
Sr. No.	Code No.	*E.Coli* MTCC 443	*Sh.Flexneri* MTCC 1457	*S.Aureus* MTCC 96	*B.Subtillis* MTCC 441
1	SDZ	125	250	200	200
2	AgSDZ	100	200	125	250